

Modelling of Helicopter Underslung Dynamics using Kane's method

Rajib Shekhar Pal *

* *Vikram Sarabhai Space Centre, Trivandrum, Kerala 695022 India*
(e-mail: rajib_shekhar@vssc.gov.in).

Abstract: The mathematical modelling of the dynamics of a helicopter underslung system consisting of multiple rigid bodies interconnected by cables is described in this paper. The differential equations of motion are derived using the matrix form of Kane's method. This avoids the enormous complexity involved in symbolic derivations, which are usually available in the published literature. The generalized coordinates and generalized speeds are selected suitably to derive the kinematical relationships describing the motion of the joints and centres of gravity of the different bodies present in the underslung system. The formulated model is validated using the principle of conservation of mechanical energy neglecting the dissipative forces. Simulation results demonstrating the characteristic motion of the system are presented.

© 2020, IFAC (International Federation of Automatic Control) Hosting by Elsevier Ltd. All rights reserved.

Keywords: Multi-body dynamics, helicopter underslung, Kane's method, generalized coordinates, modelling

1. INTRODUCTION

Orbital launch systems like the Reusable Launch Vehicle (RLV) are under active development to provide low-cost access to space (Sivan and Pandian (2018)). The robust design of such autonomous re-entry vehicles requires extensive flight tests to evaluate their onboard algorithms and landing systems. The flight trials are performed using a helicopter that releases the RLV at different locations around the runway to simulate the various approach scenarios of autonomous landing. The stability of the RLV slung underneath the helicopter is essential for the successful execution of the flight trials. This requires modelling of the constrained dynamics involving multiple rigid bodies. Most of the available literature like Thanapalan (2016), Enciu and Rosen (2014), Oktay and Sultan (2013) and Cicolani and Ehlers (2002) describe the motion of a single box-type cargo with or without fin stabilization. The experimental vehicles like RLV and ALFLEX (Tsukamoto et al. (1997)) require an additional hoist mechanism for various flight operations, as seen in Fig. 1. The complexity of modelling the dynamics of such multiple interconnected bodies surpasses the existing literature.

This paper describes the modelling of an underslung system consisting of multiple rigid bodies interconnected by cables. The constraints imposed on the dynamics due to interconnections between the bodies govern the methodology to be used for deriving the equations of motion. The formalisms described in the literature can be grouped into three major categories.

- Newton-Euler method - This method uses the full set of degrees of freedom of all the component bodies of the system, and involve the constraint forces due to each joint, which have to be found out explicitly. This method becomes intractable as the number of rigid bodies increases.

- Euler-Lagrange equations - This formalism focuses on the mechanical energy of the system to derive the equations of motion. This method uses a reduced number of coordinates, thereby imposing the motion constraints implicitly. A distinct disadvantage of this method is that it requires the derivation of the scalar Lagrange term, which can be very complex for large systems.
- Kane's method - This method is derived from D'Alembert's principle using generalized coordinates and generalized speeds. The use of partial velocities and accelerations facilitate the use of the vectorial form of the equations which are simpler to derive than the Euler-Lagrange equations and are also easier to manipulate numerically.

Kane's method is extensively used in the literature to model multi-body systems. However, most of the available literature, like Rambely et al. (2012), Purushotham and Anjeneyulu (2013) and Sandino et al. (2011), focuses on symbolic derivations which are enormously difficult for complex systems. Stoneking (2013) has presented an alternative matrix form of Kane's equation which is amenable to be used numerically, facilitating the modelling of multiple interconnected bodies. However, it does not provide for the modelling of massless rigid bodies, which may be required in certain cases. This paper addresses the derivation of motion of systems containing such massless components. The layout of the paper is as follows.

Section 2 of this paper gives a brief overview of Kane's method. Section 3 describes the assumptions used in modelling, coordinate systems involved and the derivation of the equations of motion. Section 4 gives the results of the numerical simulations using the formulated model.

1.1 Notations

The notations used in this paper for systematic representation of vector quantities in different reference frames are stated below.

- ${}^B C^A$ denotes the Direction Cosine matrix of frame A with respect to frame B .
- ${}^C \omega^{A/B}$ and ${}^C \alpha^{A/B}$ denote the angular velocity and angular acceleration respectively of the frame fixed in body A with respect to the frame fixed in body B as expressed in frame C .
- ${}^C r^{p/o}$, ${}^C v^{p/o}$ and ${}^C a^{p/o}$ denote the position, linear velocity and acceleration vectors of the point p from point o as expressed in the frame C .
- ${}^A F^B$ is the force vector identified with *name* acting on body B as expressed in the frame A .
- The moment vector denoted as ${}^A M^{B/o}$, is the moment vector identified with *name* acting on body B about the point o , as expressed in the frame A .

In certain intermediate steps of derivation, vectors are not explicitly expressed in a particular frame, and the left superscripts are omitted.

2. DESCRIPTION OF KANE'S METHOD

For a multibody system consisting of N_b rigid bodies with n degrees of freedom, Kane's equation is written as a set of scalar equations following Kane and Levinson (1985)

$$\sum_{k=1}^{N_b} [\omega_r^k \cdot (M_k - I_k \alpha_k - \omega_k \times I_k \omega_k)] + \sum_{k=1}^{N_b} [v_r^k \cdot (F_k - m_k a_k)] = 0, \quad r = 1, 2, \dots, n \quad (1)$$

where M_k and F_k are the active moments and forces acting on k^{th} rigid body respectively. ω_r^k and v_r^k are the partial angular velocity and partial linear velocity of the k^{th} rigid body with respect to the r^{th} generalized speed. α_k and ω_k are the angular acceleration and angular velocity of the k^{th} rigid body about its CG, and a_k is the respective linear acceleration of the CG. m_k is its mass, and I_k is the inertia tensor in its own body axis with respect to the CG.

Stoneking (2013) has expressed (1) into its matrix form as

$$(\Omega^T [I] \Omega + V^T [m] V) \dot{u} = \Omega^T (\{M\} - [I] \{\alpha_r\} - \{\omega\} \times [I] \{\omega\}) + V^T (\{F\} - [m] \{a_r\}) \quad (2)$$

where, Ω and V are the partial angular and linear velocity matrices. α_r and a_r are the remainder angular acceleration and linear acceleration respectively, and u is the column matrix of the generalized speeds.

3. MATHEMATICAL MODELLING

The multi-body underslung system presented in this paper is illustrated in Fig. 2. The helicopter is idealized as a point at the helicopter attachment point J_1 . Its motion is assumed to be instantaneous and unaffected by the dynamics of the underslung system. Such idealization is



Fig. 1. Underslung mechanism for helicopter trials of RLV required to design underslung configurations irrespective of the type of helicopter carrying it.

A single cable S_1 is attached at J_1 which then forks into a set of four cables S_2 at the point J_2 . The S_2 cables support the hoist mechanism, underneath which another cable S_3 is attached at the point J_3 . The cable S_3 supports the RLV by attaching at the point J_4 . All cables present in this system are assumed to be massless and always in tension. As a result, the cables S_1 and S_3 act as massless rigid links, while the cable set S_2 together with the hoist mechanism forms a rigid body. Further, the massless cables S_1 and S_3 do not rotate about their longitudinal axis and do not exhibit any torsional motion.

3.1 Coordinate Frames

The reference frames as illustrated in Fig. 2 are described as follows.

- Inertial reference frame N (X_N, Y_N, Z_N) - This Newtonian reference frame is similar to the North-East-Down frame widely used in aircraft literature. The origin is fixed at time $t = 0$ on the Earth's surface at the helicopter location. The X_N axis is in the local horizontal plane and points towards the east. Z_N axis is along the local vertical and points into the ground, and the Y_N axis completes the right-handed coordinate system.
- B_1 frame (X_{B1}, Y_{B1}, Z_{B1}) - This reference frame is attached to the massless rigid cable S_1 . The Z_{B1} axis is along the length of the cable pointing downwards away from J_1 .
- B_2 frame (X_{B2}, Y_{B2}, Z_{B2}) - This reference frame is attached to the rigid body consisting of the hoist mechanism along with the cables S_2 . Its centre of mass is at the point O_2 .

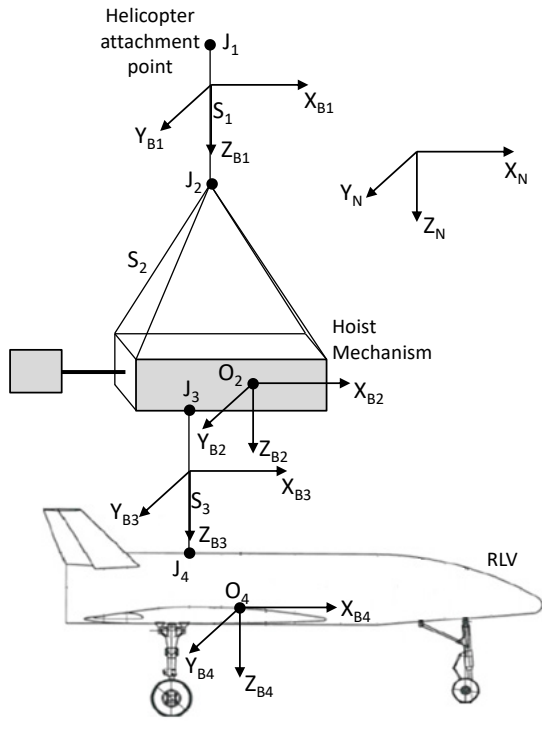


Fig. 2. Illustration of Coordinate frames

- B_3 frame (X_{B3}, Y_{B3}, Z_{B3}) - The massless cable S_3 connecting the hoist mechanism to the RLV contains the B_3 frame. The Z_{B3} axis is along the length of the cable pointing downwards away from J_3 .
- B_4 frame (X_{B4}, Y_{B4}, Z_{B4}) - This reference frame is attached to the RLV at its CG, which is indicated by the point O_4 in Fig. 2.

3.2 Derivation of Equations of Motion

The degrees of freedom for this multi-body system can be ascertained as follows.

- The motion of the helicopter which is idealized as the massless point J_1 has 3 translational degrees of freedom in the inertial space, given by ${}^N\mathbf{r}_0 = (x_0, y_0, z_0)$.
- The massless body B_1 has 2 rotational degrees of freedom about the joint J_1 , denoted by the joint angles θ_{11} and θ_{12} . Following the rotation sequence $\phi_y \rightarrow \phi_x$ the transformation from the N frame to the B_1 frame is represented by

$$N \xrightarrow[\text{by } \theta_{11}]{\text{about } Y} B'_1 \xrightarrow[\text{by } \theta_{12}]{\text{about } X} B_1$$

- The rigid body B_2 has 3 rotational degrees of freedom about the joint J_2 , denoted by the joint angles θ_{21} , θ_{22} and θ_{23} . Following the rotation sequence $\phi_y \rightarrow \phi_x \rightarrow \phi_z$, the transformation from the B_1 frame to the B_2 frame is represented by

$$B_1 \xrightarrow[\text{by } \theta_{21}]{\text{about } Y} B'_2 \xrightarrow[\text{by } \theta_{22}]{\text{about } X} B''_2 \xrightarrow[\text{by } \theta_{23}]{\text{about } Z} B_2$$

- Similar to B_1 , the massless body B_3 has 2 rotational degrees of freedom about the joint J_3 . These are denoted by the joint angles θ_{31} and θ_{32} . The transformation from the B_2 frame to the B_3 frame is represented by

$$B_2 \xrightarrow[\text{by } \theta_{31}]{\text{about } Y} B'_3 \xrightarrow[\text{by } \theta_{32}]{\text{about } X} B_3$$

- Lastly, the rigid body B_4 has 3 rotational degrees of freedom about the joint J_4 , which are denoted by the joint angles θ_{41} , θ_{42} and θ_{43} . The transformation from the B_3 frame to the B_4 frame is represented by

$$B_3 \xrightarrow[\text{by } \theta_{41}]{\text{about } Y} B'_4 \xrightarrow[\text{by } \theta_{42}]{\text{about } X} B''_4 \xrightarrow[\text{by } \theta_{43}]{\text{about } Z} B_4$$

Following the described Euler angle sequences, the transformation matrices between different frames can be established as per Henderson (1977).

The relationships between the angular body rates (ω) and the joint angular rates (σ) are derived from the kinematical relationships involving the derivatives of Euler angles. Writing the joint angle rates in column vectors,

$$\begin{aligned} \sigma_1 &= \begin{Bmatrix} \sigma_{11} \\ \sigma_{12} \end{Bmatrix} = \begin{Bmatrix} \dot{\theta}_{11} \\ \dot{\theta}_{12} \end{Bmatrix} & \sigma_2 &= \begin{Bmatrix} \sigma_{21} \\ \sigma_{22} \\ \sigma_{23} \end{Bmatrix} = \begin{Bmatrix} \dot{\theta}_{21} \\ \dot{\theta}_{22} \\ \dot{\theta}_{23} \end{Bmatrix} \\ \sigma_3 &= \begin{Bmatrix} \sigma_{31} \\ \sigma_{32} \end{Bmatrix} = \begin{Bmatrix} \dot{\theta}_{31} \\ \dot{\theta}_{32} \end{Bmatrix} & \sigma_4 &= \begin{Bmatrix} \sigma_{41} \\ \sigma_{42} \\ \sigma_{43} \end{Bmatrix} = \begin{Bmatrix} \dot{\theta}_{41} \\ \dot{\theta}_{42} \\ \dot{\theta}_{43} \end{Bmatrix} \end{aligned} \quad (3)$$

the angular body rates ${}^1\omega^{1/N}$, ${}^2\omega^{2/1}$, ${}^3\omega^{3/2}$ and ${}^4\omega^{4/3}$ can be represented as the following

$${}^1\omega^{1/N} = \Gamma_1 \sigma_1 \quad (4a)$$

$${}^2\omega^{2/1} = \Gamma_2 \sigma_2 \quad (4b)$$

$${}^3\omega^{3/2} = \Gamma_3 \sigma_3 \quad (4c)$$

$${}^4\omega^{4/3} = \Gamma_4 \sigma_4 \quad (4d)$$

where,

$$\Gamma_1 = \begin{bmatrix} 0 & 1 \\ \cos \theta_{12} & 0 \\ -\sin \theta_{12} & 0 \end{bmatrix} \quad (5a)$$

$$\Gamma_2 = \begin{bmatrix} \cos \theta_{22} \sin \theta_{23} & \cos \theta_{23} & 0 \\ \cos \theta_{22} \cos \theta_{23} & -\sin \theta_{23} & 0 \\ -\sin \theta_{22} & 0 & 1 \end{bmatrix} \quad (5b)$$

$$\Gamma_3 = \begin{bmatrix} 0 & 1 \\ \cos \theta_{32} & 0 \\ -\sin \theta_{32} & 0 \end{bmatrix} \quad (5c)$$

$$\Gamma_4 = \begin{bmatrix} \cos \theta_{42} \sin \theta_{43} & \cos \theta_{43} & 0 \\ \cos \theta_{42} \cos \theta_{43} & -\sin \theta_{43} & 0 \\ -\sin \theta_{42} & 0 & 1 \end{bmatrix} \quad (5d)$$

The angular velocities of the rigid bodies B_2 and B_4 with respect to N are expressed in their respective frames as

$$\begin{aligned} {}^2\omega^{2/N} &= {}^2C^{11}\omega^{1/N} + {}^2\omega^{2/1} \\ &= {}^2C^1\Gamma_1 \sigma_1 + \Gamma_2 \sigma_2 \end{aligned} \quad (6a)$$

$$\begin{aligned} {}^4\omega^{4/N} &= {}^4C^{11}\omega^{1/N} + {}^4C^{22}\omega^{2/1} + {}^4C^{33}\omega^{3/2} + {}^4\omega^{4/3} \\ &= {}^4C^1\Gamma_1 \sigma_1 + {}^4C^2\Gamma_2 \sigma_2 + {}^4C^3\Gamma_3 \sigma_3 + \Gamma_4 \sigma_4 \end{aligned} \quad (6b)$$

Equation (6) can be grouped together into a system of identities to form the *partial angular velocity matrix* Ω .

$$\begin{bmatrix} {}^2\boldsymbol{\omega}^{2/N} \\ {}^4\boldsymbol{\omega}^{4/N} \end{bmatrix} = \underbrace{\begin{bmatrix} {}^2C^1\Gamma_1 & \Gamma_2 & 0 & 0 \\ {}^4C^1\Gamma_1 & {}^4C^2\Gamma_2 & {}^4C^3\Gamma_3 & \Gamma_4 \end{bmatrix}}_{\Omega} \begin{bmatrix} \sigma_1 \\ \sigma_2 \\ \sigma_3 \\ \sigma_4 \end{bmatrix} \quad (7)$$

Next, the angular acceleration of the B_1 body with respect to frame N is derived.

$$\boldsymbol{\alpha}^{1/N} = \frac{d}{dt} {}^{1/N}\boldsymbol{\omega}^{1/N} = \frac{d}{dt} {}^{1/1}\boldsymbol{\omega}^{1/N} + {}^{1/N}\boldsymbol{\omega}^{1/N} \times {}^{1/N}\boldsymbol{\omega}^{1/N} \quad (8)$$

where, $\frac{d}{dt} {}^{1/N}$ and $\frac{d}{dt} {}^{1/1}$ denote the time derivative in frames N and B_1 respectively.

The vector $\boldsymbol{\alpha}^{1/N}$ can be expressed in the B_1 frame as

$${}^1\boldsymbol{\alpha}^{1/N} = {}^1\dot{\boldsymbol{\omega}}^{1/N} = \Gamma_1\dot{\sigma}_1 + \dot{\Gamma}_1\sigma_1 = \Gamma_1\dot{\sigma}_1 + {}^1\boldsymbol{\alpha}_r^{1/N} \quad (9)$$

where ${}^1\boldsymbol{\alpha}_r^{1/N}$ is the *remainder angular acceleration* following the terminology of Stoneking (2013), and $\dot{\Gamma}_1$ is the time derivative of Γ_1 .

$${}^1\boldsymbol{\alpha}_r^{1/N} = \dot{\Gamma}_1\sigma_1 \quad (10a)$$

$$\dot{\Gamma}_1 = \begin{bmatrix} 0 & 0 \\ -\sigma_{12}\sin\theta_{12} & 0 \\ -\sigma_{12}\cos\theta_{12} & 0 \end{bmatrix} \quad (10b)$$

Similarly, the angular acceleration $\boldsymbol{\alpha}^{2/N}$ is derived.

$$\begin{aligned} \boldsymbol{\alpha}^{2/N} &= \frac{d}{dt} {}^{1/N}\boldsymbol{\omega}^{2/N} = \frac{d}{dt} {}^{1/2}\boldsymbol{\omega}^{2/N} + {}^{1/N}\boldsymbol{\omega}^{2/N} \times {}^{1/N}\boldsymbol{\omega}^{2/N} \\ &= \frac{d}{dt} {}^{1/1}\boldsymbol{\omega}^{1/N} + {}^{1/2}\boldsymbol{\omega}^{1/2} \times {}^{1/N}\boldsymbol{\omega}^{1/N} + \dot{\boldsymbol{\omega}}^{2/1} \\ &= \dot{\boldsymbol{\omega}}^{1/N} + \dot{\boldsymbol{\omega}}^{2/1} + {}^{1/N}\boldsymbol{\omega}^{1/N} \times {}^{2/1}\boldsymbol{\omega}^{2/1} \end{aligned} \quad (11)$$

The vector $\boldsymbol{\alpha}^{2/N}$ can be expressed in the B_2 frame as

$$\begin{aligned} {}^2\boldsymbol{\alpha}^{2/N} &= {}^2C^{11}\dot{\boldsymbol{\omega}}^{1/N} + {}^2\dot{\boldsymbol{\omega}}^{2/1} + \left({}^2C^{11}{}^1\boldsymbol{\omega}^{1/N}\right) \times {}^2\boldsymbol{\omega}^{2/1} \\ &= {}^2C^1\left(\Gamma_1\dot{\sigma}_1 + {}^1\boldsymbol{\alpha}_r^{1/N}\right) + \Gamma_2\dot{\sigma}_2 + \dot{\Gamma}_2\sigma_2 \\ &\quad + \left({}^2C^{11}{}^1\boldsymbol{\omega}^{1/N}\right) \times {}^2\boldsymbol{\omega}^{2/1} \\ &= {}^2C^1\Gamma_1\dot{\sigma}_1 + \Gamma_2\dot{\sigma}_2 + {}^2\boldsymbol{\alpha}_r^{2/N} \end{aligned} \quad (12)$$

where,

$${}^2\boldsymbol{\alpha}_r^{2/N} = {}^2C^{11}{}^1\boldsymbol{\alpha}_r^{1/N} + \dot{\Gamma}_2\sigma_2 + \left({}^2C^{11}{}^1\boldsymbol{\omega}^{1/N}\right) \times {}^2\boldsymbol{\omega}^{2/1} \quad (13a)$$

$$\dot{\Gamma}_2 = \begin{bmatrix} -\sigma_{22}\sin\theta_{22}\sin\theta_{23} + \sigma_{23}\cos\theta_{22}\cos\theta_{23} & -\sigma_{23}\sin\theta_{23} & 0 \\ -\sigma_{22}\sin\theta_{22}\cos\theta_{23} - \sigma_{23}\cos\theta_{22}\sin\theta_{23} & -\sigma_{23}\cos\theta_{23} & 0 \\ -\sigma_{22}\cos\theta_{22} & 0 & 0 \end{bmatrix} \quad (13b)$$

Similar expressions can be found out for the angular accelerations of bodies B_3 and B_4 . For the body B_3 ,

$${}^3\boldsymbol{\alpha}^{3/N} = {}^3C^1\Gamma_1\dot{\sigma}_1 + {}^3C^2\Gamma_2\dot{\sigma}_2 + \Gamma_3\dot{\sigma}_3 + {}^3\boldsymbol{\alpha}_r^{3/N} \quad (14a)$$

$${}^3\boldsymbol{\alpha}_r^{3/N} = {}^3C^2{}^2\boldsymbol{\alpha}_r^{2/N} + \dot{\Gamma}_3\sigma_3 + \left({}^3C^2{}^2\boldsymbol{\omega}^{2/N}\right) \times {}^3\boldsymbol{\omega}^{3/2} \quad (14b)$$

$$\dot{\Gamma}_3 = \begin{bmatrix} 0 & 0 \\ -\sigma_{32}\sin\theta_{32} & 0 \\ -\sigma_{32}\cos\theta_{32} & 0 \end{bmatrix} \quad (14c)$$

For the body B_4 ,

$${}^4\boldsymbol{\alpha}^{4/N} = {}^4C^1\Gamma_1\dot{\sigma}_1 + {}^4C^2\Gamma_2\dot{\sigma}_2 + {}^4C^3\Gamma_3\dot{\sigma}_3 + \Gamma_4\dot{\sigma}_4 + {}^4\boldsymbol{\alpha}_r^{4/N} \quad (15a)$$

$${}^4\boldsymbol{\alpha}_r^{4/N} = {}^4C^3{}^3\boldsymbol{\alpha}_r^{3/N} + \dot{\Gamma}_4\sigma_4 + \left({}^4C^3{}^3\boldsymbol{\omega}^{3/N}\right) \times {}^4\boldsymbol{\omega}^{4/3} \quad (15b)$$

$$\dot{\Gamma}_4 = \begin{bmatrix} -\sigma_{42}\sin\theta_{42}\sin\theta_{43} + \sigma_{43}\cos\theta_{42}\cos\theta_{43} & -\sigma_{43}\sin\theta_{43} & 0 \\ -\sigma_{42}\sin\theta_{42}\cos\theta_{43} - \sigma_{43}\cos\theta_{42}\sin\theta_{43} & -\sigma_{43}\cos\theta_{43} & 0 \\ -\sigma_{42}\cos\theta_{42} & 0 & 0 \end{bmatrix} \quad (15c)$$

Next, the position of the points $J_1, J_2, O_2, J_3, J_4, O_4$ are computed in N . The position vector of the point J_1 with respect to n , a point fixed in the inertial frame N is

$${}^N\boldsymbol{r}^{J_1/n} = {}^N\boldsymbol{r}_0 \quad (16)$$

where, \boldsymbol{r}_0 is the position vector of the helicopter attachment point J_1 , given as input.

The position vectors of the rest of the points with respect to the point n are

$${}^N\boldsymbol{r}^{J_2/n} = {}^N\boldsymbol{r}^{J_1/n} - {}^N\boldsymbol{C}^{11}\boldsymbol{r}^{J_1/J_2} \quad (17a)$$

$${}^N\boldsymbol{r}^{O_2/n} = {}^N\boldsymbol{r}^{J_2/n} - {}^N\boldsymbol{C}^{22}\boldsymbol{r}^{J_2/O_2} \quad (17b)$$

$${}^N\boldsymbol{r}^{J_3/n} = {}^N\boldsymbol{r}^{O_2/n} + {}^N\boldsymbol{C}^{22}\boldsymbol{r}^{J_3/O_2} \quad (17c)$$

$${}^N\boldsymbol{r}^{J_4/n} = {}^N\boldsymbol{r}^{J_3/n} - {}^N\boldsymbol{C}^{33}\boldsymbol{r}^{J_3/J_4} \quad (17d)$$

$${}^N\boldsymbol{r}^{O_4/n} = {}^N\boldsymbol{r}^{J_4/n} - {}^N\boldsymbol{C}^{44}\boldsymbol{r}^{J_4/O_4} \quad (17e)$$

where, ${}^1\boldsymbol{r}^{J_1/J_2}, {}^2\boldsymbol{r}^{J_2/O_2}, {}^2\boldsymbol{r}^{J_3/O_2}, {}^3\boldsymbol{r}^{J_3/J_4}$ and ${}^4\boldsymbol{r}^{J_4/O_4}$ are given as inputs.

Next, the velocity of the point J_1 is computed as

$${}^N\boldsymbol{v}^{J_1/n} = {}^N\boldsymbol{v}_0 = \frac{d}{dt} {}^N\boldsymbol{r}_0 \quad (18)$$

The velocity of the point O_2 is derived as

$$\begin{aligned} \boldsymbol{v}^{O_2/n} &= \boldsymbol{v}^{J_1/n} + \boldsymbol{\omega}^{1/N} \times \boldsymbol{r}^{J_2/J_1} + \boldsymbol{\omega}^{2/N} \times \boldsymbol{r}^{O_2/J_2} \\ &= \boldsymbol{v}^{J_1/n} + \boldsymbol{\omega}^{1/N} \times \left(\boldsymbol{r}^{J_2/J_1} + \boldsymbol{r}^{O_2/J_2} \right) \\ &\quad + \boldsymbol{\omega}^{2/1} \times \boldsymbol{r}^{O_2/J_2} \\ &= \boldsymbol{v}^{J_1/n} + \boldsymbol{r}^{J_1/O_2} \times \boldsymbol{\omega}^{1/N} + \boldsymbol{r}^{J_2/O_2} \times \boldsymbol{\omega}^{2/1} \end{aligned} \quad (19)$$

When expressed in the inertial frame N , (19) is written as

$$\begin{aligned} {}^N\boldsymbol{v}^{O_2/n} &= {}^N\boldsymbol{v}^{J_1/n} + {}^N\boldsymbol{r}^{J_1/O_2} \times {}^N\boldsymbol{C}^{11}\boldsymbol{\omega}^{1/N} \\ &\quad + {}^N\boldsymbol{r}^{J_2/O_2} \times {}^N\boldsymbol{C}^{22}\boldsymbol{\omega}^{2/1} \\ &= {}^N\boldsymbol{v}_0 + {}^N\boldsymbol{r}^{J_1/O_2} \times {}^N\boldsymbol{C}^{11}\Gamma_1\sigma_1 \\ &\quad + {}^N\boldsymbol{r}^{J_2/O_2} \times {}^N\boldsymbol{C}^{22}\Gamma_2\sigma_2 \end{aligned} \quad (20)$$

The velocity of the point O_4 can be similarly derived in the frame N as

$$\begin{aligned} {}^N\boldsymbol{v}^{O_4/n} &= {}^N\boldsymbol{v}_0 + {}^N\boldsymbol{r}^{J_1/O_4} \times {}^N\boldsymbol{C}^{11}\Gamma_1\sigma_1 \\ &\quad + {}^N\boldsymbol{r}^{J_2/O_4} \times {}^N\boldsymbol{C}^{22}\Gamma_2\sigma_2 \\ &\quad + {}^N\boldsymbol{r}^{J_3/O_4} \times {}^N\boldsymbol{C}^{33}\Gamma_3\sigma_3 + {}^N\boldsymbol{r}^{J_4/O_4} \times {}^N\boldsymbol{C}^{44}\Gamma_4\sigma_4 \end{aligned} \quad (21)$$

Equations (20) and (21) can be grouped to form the *partial velocity matrix* V as

$$\begin{bmatrix} {}^N\mathbf{v}^{O_2/n} \\ {}^N\mathbf{v}^{O_4/n} \end{bmatrix} = V \begin{bmatrix} \sigma_1 \\ \sigma_2 \\ \sigma_3 \\ \sigma_4 \end{bmatrix} + \begin{bmatrix} {}^N\mathbf{v}_0 \\ {}^N\mathbf{v}_0 \end{bmatrix} \quad (22a)$$

$$V^T = \begin{bmatrix} {}^N\mathbf{r}_\times^{J_1/O_2} {}^N\mathbf{C}^1\Gamma_1 & {}^N\mathbf{r}_\times^{J_1/O_4} {}^N\mathbf{C}^1\Gamma_1 \\ {}^N\mathbf{r}_\times^{J_2/O_2} {}^N\mathbf{C}^2\Gamma_2 & {}^N\mathbf{r}_\times^{J_2/O_4} {}^N\mathbf{C}^2\Gamma_2 \\ 0 & {}^N\mathbf{r}_\times^{J_3/O_4} {}^N\mathbf{C}^3\Gamma_3 \\ 0 & {}^N\mathbf{r}_\times^{J_4/O_4} {}^N\mathbf{C}^4\Gamma_4 \end{bmatrix} \quad (22b)$$

${}^N\mathbf{r}_\times^{J_1/O_2}$ and other similar terms in (22b) are skew-symmetric matrices. As an example, a_\times is a skew-symmetric matrix of vector \mathbf{a} such that $\mathbf{a} \times \mathbf{b} = a_\times \mathbf{b}$.

Now, the acceleration of the points O_2 and O_4 , which are the centers of gravity of the rigid bodies B_2 and B_4 respectively, are derived. The acceleration of point O_2 is computed as

$$\begin{aligned} {}^N\mathbf{a}^{O_2/n} &= {}^N\mathbf{a}^{J_1/n} + \alpha^{1/N} \times {}^N\mathbf{r}^{J_2/J_1} + \omega^{1/N} \times (\omega^{1/N} \times {}^N\mathbf{r}^{J_2/J_1}) \\ &\quad + \alpha^{2/N} \times {}^N\mathbf{r}^{O_2/J_2} + \omega^{2/N} \times (\omega^{2/N} \times {}^N\mathbf{r}^{O_2/J_2}) \end{aligned} \quad (23)$$

Expressed in inertial frame N , (23) can be written as

$$\begin{aligned} {}^N\mathbf{a}^{O_2/n} &= {}^N\mathbf{a}^{J_1/n} + {}^N\mathbf{C}^{11}\alpha^{1/N} \times {}^N\mathbf{r}^{J_2/J_1} \\ &\quad + {}^N\mathbf{C}^{22}\alpha^{2/N} \times {}^N\mathbf{r}^{O_2/J_2} \\ &\quad + \omega^{1/N} \times (\omega^{1/N} \times {}^N\mathbf{r}^{J_2/J_1}) \\ &\quad + \omega^{2/N} \times (\omega^{2/N} \times {}^N\mathbf{r}^{O_2/J_2}) \end{aligned} \quad (24)$$

where, ${}^N\omega^{1/N} = {}^N\mathbf{C}^{11}\omega^{1/N}$ and ${}^N\omega^{2/N} = {}^N\mathbf{C}^{22}\omega^{2/N}$

Substituting (10a) and (13a) in (24), we get

$$\begin{aligned} {}^N\mathbf{a}^{O_2/n} &= {}^N\mathbf{a}_0 + {}^N\mathbf{C}^1 (\Gamma_1\dot{\sigma}_1 + {}^1\alpha_r^{1/N}) \times {}^N\mathbf{r}^{J_2/J_1} \\ &\quad + {}^N\mathbf{C}^2 ({}^2\mathbf{C}^1\Gamma_1\dot{\sigma}_1 + \Gamma_2\dot{\sigma}_2 + {}^2\alpha_r^{2/N}) \times {}^N\mathbf{r}^{O_2/J_2} \\ &\quad + \omega^{1/N} \times (\omega^{1/N} \times {}^N\mathbf{r}^{J_2/J_1}) \\ &\quad + \omega^{2/N} \times (\omega^{2/N} \times {}^N\mathbf{r}^{O_2/J_2}) \\ &= {}^N\mathbf{C}^1\Gamma_1\dot{\sigma}_1 \times {}^N\mathbf{r}^{J_2/J_1} + {}^N\mathbf{C}^1\Gamma_1\dot{\sigma}_1 \times {}^N\mathbf{r}^{O_2/J_2} \\ &\quad + {}^N\mathbf{C}^2\Gamma_2\dot{\sigma}_2 \times {}^N\mathbf{r}^{O_2/J_2} + {}^N\mathbf{a}_r^{O_2/n} \\ &= {}^N\mathbf{r}^{J_1/O_2} \times {}^N\mathbf{C}^1\Gamma_1\dot{\sigma}_1 + {}^N\mathbf{r}^{J_2/O_2} \times {}^N\mathbf{C}^2\Gamma_2\dot{\sigma}_2 \\ &\quad + {}^N\mathbf{a}_r^{O_2/n} \end{aligned} \quad (25)$$

where, the remainder acceleration ${}^N\mathbf{a}_r^{O_2/n}$ is

$$\begin{aligned} {}^N\mathbf{a}_r^{O_2/n} &= {}^N\mathbf{a}_0 + {}^N\mathbf{C}^{11}\alpha_r^{1/N} \times {}^N\mathbf{r}^{J_2/J_1} \\ &\quad + {}^N\mathbf{C}^{22}\alpha_r^{2/N} \times {}^N\mathbf{r}^{O_2/J_2} \\ &\quad + \omega^{1/N} \times (\omega^{1/N} \times {}^N\mathbf{r}^{J_2/J_1}) \\ &\quad + \omega^{2/N} \times (\omega^{2/N} \times {}^N\mathbf{r}^{O_2/J_2}) \end{aligned} \quad (26)$$

Similar expression can be written for the acceleration of point O_4 using (25), (12), (14a) and (15a).

$$\begin{aligned} {}^N\mathbf{a}^{O_4/n} &= {}^N\mathbf{r}^{J_1/O_4} \times {}^N\mathbf{C}^1\Gamma_1\dot{\sigma}_1 + {}^N\mathbf{r}^{J_2/O_4} \times {}^N\mathbf{C}^2\Gamma_2\dot{\sigma}_2 \\ &\quad + {}^N\mathbf{r}^{J_3/O_4} \times {}^N\mathbf{C}^3\Gamma_3\dot{\sigma}_3 + {}^N\mathbf{r}^{J_4/O_4} \times {}^N\mathbf{C}^4\Gamma_4\dot{\sigma}_4 \\ &\quad + {}^N\mathbf{a}_r^{O_4/n} \end{aligned} \quad (27)$$

where, the remainder acceleration ${}^N\mathbf{a}_r^{O_4/n}$ is

$$\begin{aligned} {}^N\mathbf{a}_r^{O_4/n} &= {}^N\mathbf{a}_r^{O_2/n} + {}^N\mathbf{r}^{O_2/J_3} \times {}^N\mathbf{C}^{22}\alpha_r^{2/N} \\ &\quad + {}^N\mathbf{r}^{J_3/J_4} \times {}^N\mathbf{C}^{33}\alpha_r^{3/N} \\ &\quad + {}^N\mathbf{r}^{J_4/O_4} \times {}^N\mathbf{C}^{44}\alpha_r^{4/N} \\ &\quad + \omega^{2/N} \times (\omega^{2/N} \times {}^N\mathbf{r}^{J_3/O_2}) \\ &\quad + \omega^{3/N} \times (\omega^{3/N} \times {}^N\mathbf{r}^{J_4/J_3}) \\ &\quad + \omega^{4/N} \times (\omega^{4/N} \times {}^N\mathbf{r}^{O_4/J_4}) \end{aligned} \quad (28)$$

The active forces and moments acting on the rigid bodies B_2 and B_4 are the gravitational force and the aerodynamic forces and moments. Following the expressions of the translational and rotational accelerations, the active forces are expressed in the inertial frame, while the active moments are expressed in the frames of the bodies on which they act, about their respective centres of gravity. For body B_2 , the active forces and moments acting are

$${}^N\mathbf{F}^{B_2} = {}^N\mathbf{F}_G^{B_2} + {}^N\mathbf{F}_A^{B_2} \quad (29a)$$

$${}^2\mathbf{M}^{B_2/O_2} = {}^2\mathbf{M}_A^{B_2/O_2} \quad (29b)$$

and for body B_4 they are

$${}^N\mathbf{F}^{B_4} = {}^N\mathbf{F}_G^{B_4} + {}^N\mathbf{F}_A^{B_4} \quad (30a)$$

$${}^4\mathbf{M}^{B_4/O_4} = {}^4\mathbf{M}_A^{B_4/O_4} \quad (30b)$$

where, \mathbf{F}_G and \mathbf{F}_A are the gravitational force and aerodynamic force respectively, and \mathbf{M}_A is the aerodynamic moment. Under the assumption of flat Earth, the gravitational forces are computed in the inertial frame N as

$${}^N\mathbf{F}_G^{B_2} = \begin{Bmatrix} 0 \\ 0 \\ m_2 g \end{Bmatrix} \quad {}^N\mathbf{F}_G^{B_4} = \begin{Bmatrix} 0 \\ 0 \\ m_4 g \end{Bmatrix} \quad (31)$$

where, m_2 and m_4 are the masses of the bodies B_2 and B_4 respectively, and g is the acceleration due to gravity.

To form the system of differential equations as per (2), the Ω and V matrices are derived in equations (7) and (22b) respectively. The remaining terms $\{m\}$, $\{I\}$, $\{\omega\}$, $\{\alpha_r\}$, $\{a_r\}$, $\{F\}$ and $\{M\}$ are derived as

$$[m] = \begin{bmatrix} m_2 U_{3 \times 3} & 0 \\ 0 & m_4 U_{3 \times 3} \end{bmatrix} \quad [I] = \begin{bmatrix} I^{B_2/O_2} & 0 \\ 0 & I^{B_4/O_4} \end{bmatrix} \quad (32a)$$

$$\{\omega\} = \begin{Bmatrix} {}^2\omega^{2/N} \\ {}^4\omega^{4/N} \end{Bmatrix} \quad \{\alpha_r\} = \begin{Bmatrix} {}^2\alpha_r^{2/N} \\ {}^4\alpha_r^{4/N} \end{Bmatrix} \quad (32b)$$

$$\{a_r\} = \begin{Bmatrix} {}^N\mathbf{a}_r^{O_2/n} \\ {}^N\mathbf{a}_r^{O_4/n} \end{Bmatrix} \quad (32c)$$

$$\{F\} = \begin{Bmatrix} {}^N\mathbf{F}^{B_2} \\ {}^N\mathbf{F}^{B_4} \end{Bmatrix} \quad \{M\} = \begin{Bmatrix} {}^2\mathbf{M}^{B_2/O_2} \\ {}^4\mathbf{M}^{B_4/O_4} \end{Bmatrix} \quad (32d)$$

where, I^{B_2/O_2} and I^{B_4/O_4} are the inertia matrices in their body frames about the respective centres of gravity O_2 and O_4 . $U_{3 \times 3}$ is the unity matrix.

All the above terms are finally assembled according to (2) to form the following system of differential equations

$$[\mathbb{M}] \{\dot{\sigma}\} = \{\mathbb{F}\} \quad (33)$$

where, $[\mathbb{M}]$ is the generalized mass-matrix and the $\{\mathbb{F}\}$ is the generalized force.

4. NUMERICAL ANALYSIS

The numerical simulations of the formulated model are described in this section. The system of differential equations derived in (33) is solved at each instant using the LU-decomposition method to get the joint angular accelerations $\dot{\sigma}$. These are integrated using the Runge-Kutta 4th order scheme to obtain the joint angular speeds σ and the joint angles θ . The simulations presented here include only the effects of gravitational forces ($\mathbf{F}_G^{B_2}$ and $\mathbf{F}_G^{B_4}$) acting on the rigid bodies B_2 and B_4 , while the forces and moments due to aerodynamics are neglected. The absence of the dissipative aerodynamic forces and moments leads to the conservation of mechanical energy. This fact can be used to validate the formulated model. Furthermore, it enables in understanding the model characteristics without the external disturbances caused by aerodynamics, which is applicable at very low speeds of the helicopter. Table 1 gives the parameters used for simulation.

Table 1. Parameters used in simulations

Parameters	Value
g	$9.80665 \text{ m} \cdot \text{s}^{-2}$
m_2	1000 kg
m_4	1500 kg
$I_{xx}^{B_2/O_2}$	$430 \text{ kg} \cdot \text{m}^2$
$I_{yy}^{B_2/O_2}$	$2700 \text{ kg} \cdot \text{m}^2$
$I_{zz}^{B_2/O_2}$	$2900 \text{ kg} \cdot \text{m}^2$
$I_{xz}^{B_2/O_2}$	$120 \text{ kg} \cdot \text{m}^2$
$I_{xx}^{B_4/O_4}$	$650 \text{ kg} \cdot \text{m}^2$
$I_{yy}^{B_4/O_4}$	$4000 \text{ kg} \cdot \text{m}^2$
$I_{zz}^{B_4/O_4}$	$4400 \text{ kg} \cdot \text{m}^2$
$I_{xz}^{B_4/O_4}$	$200 \text{ kg} \cdot \text{m}^2$
${}^1\mathbf{r}_{J_1/J_2}$	$(0, 0, -5) \text{ m}$
${}^2\mathbf{r}_{J_2/O_2}$	$(0, 0, -15) \text{ m}$
${}^2\mathbf{r}_{J_3/O_2}$	$(0.1, 0, 0) \text{ m}$
${}^2\mathbf{r}_{J_3/J_4}$	$(0, 0, -5) \text{ m}$
${}^4\mathbf{r}_{J_4/O_4}$	$(0, 0, -0.7) \text{ m}$

Fig. 3, 4, 5 and 6 show the joint angles for J_1 , J_2 , J_3 and J_4 respectively, with the initial conditions of $\theta_{11} = 10^\circ$, $\theta_{42} = 10^\circ$ and ${}^N\mathbf{a}_0 = \mathbf{0}$. The integration step size is fixed as 10^{-3} s . As evident from Fig. 3 and 4, the bodies B_1 and B_2 oscillates nearly together about the joint J_1 . The pitch and roll oscillations about the joint J_2 have very small amplitudes but are of high frequency. The high frequency of oscillations is due to the massless cable B_1 , which does not impart any inertial resistance. However, the rigid body B_2 by virtue of its rotational inertia produces differential rotations between B_1 and B_2 . Despite the fact that the initial conditions do not include any rotation about yaw, the joint angles θ_{23} and θ_{43} oscillate, as seen in Fig. 4 and 6, representing yaw motion of the rigid bodies B_2 and B_4 . This is due to the non-zero products of inertia $I_{xz}^{B_2/O_2}$ and $I_{xz}^{B_4/O_4}$ as well as the small offset present in the location of joint J_3 from O_2 . Fig. 7 shows the different characteristic frequencies present in the system, as observed in the angular body rates of the body B_4 . It is evident that the low frequencies less than 1 Hz dominate

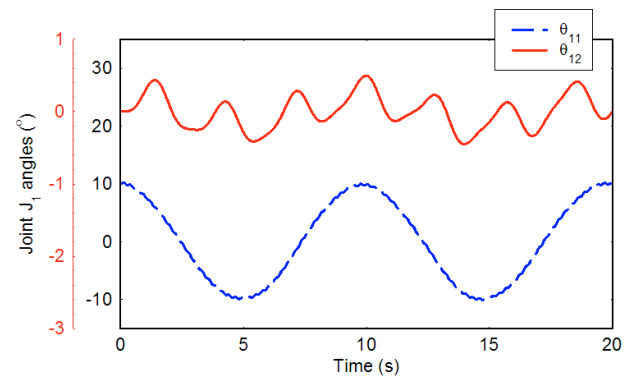


Fig. 3. Joint angles for J_1

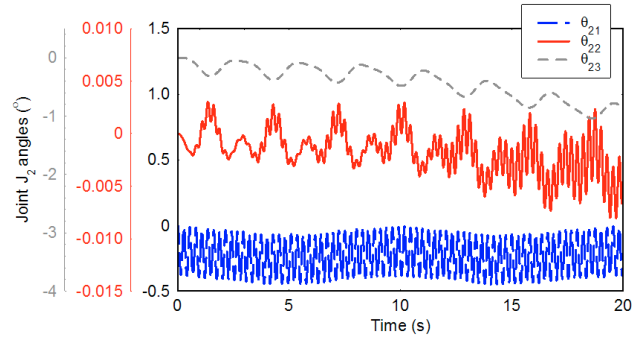


Fig. 4. Joint angles for J_2

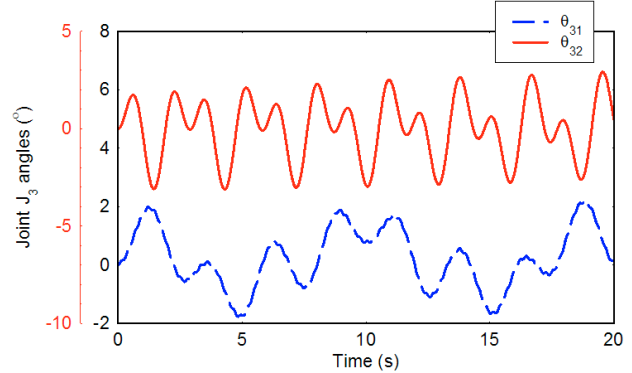


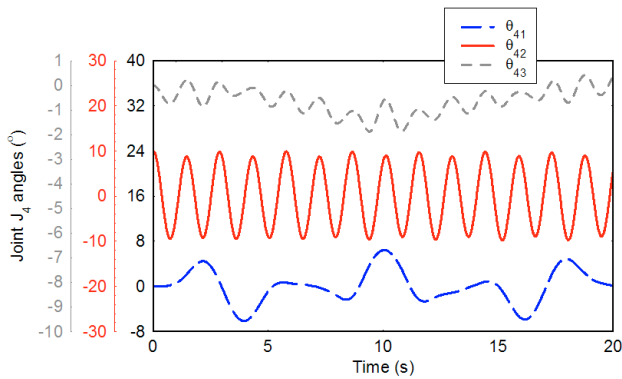
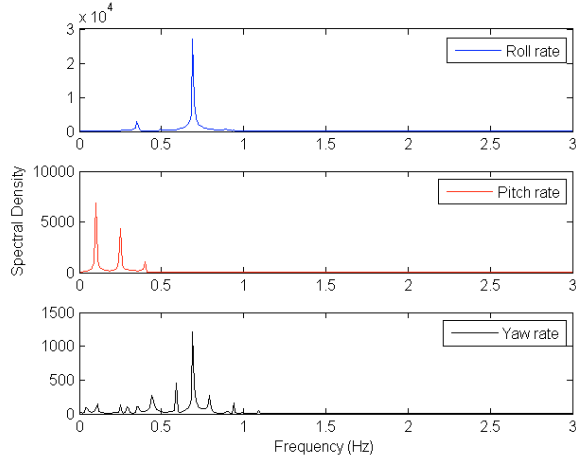
Fig. 5. Joint angles for J_3

the majority of the frequency spectrum. This is due to the large inertia of the bodies B_2 and B_4 as well as the lengths of the cables involved in this particular configuration of the underslung system.

The total mechanical energy of the system is computed as

$$E = \frac{1}{2}m_2||\mathbf{v}^{O_2/n}||^2 + \frac{1}{2}{}^N\boldsymbol{\omega}^{2/N} \cdot (I^{B_2/O_2} {}^N\boldsymbol{\omega}^{2/N}) + \frac{1}{2}m_4||\mathbf{v}^{O_4/n}||^2 + \frac{1}{2}{}^N\boldsymbol{\omega}^{4/N} \cdot (I^{B_4/O_4} {}^N\boldsymbol{\omega}^{4/N}) + m_2g(-{}^N\mathbf{r}_z^{O_2/n}) + m_4g(-{}^N\mathbf{r}_z^{O_4/n}) \quad (34)$$

The negative signs in the potential energy terms are due to the fact that gravitational acceleration acts along the positive Z_N direction. Table 2 shows a comparison of the maximum numerical error incurred for different integration step sizes during 100 s in terms of $E - E_0$, where E_0 is the mechanical energy at $t = 0$. The numerical error

Fig. 6. Joint angles for J_4 Fig. 7. Frequency response of angular body rate of B_4

is close to 0, which verifies the conservation of mechanical energy in the system. Further, the error decreases with decreasing step size, and is within 10^{-6} for step sizes of 10^{-3} s and less, which is the maximum step size tolerable.

Table 2. Numerical error incurred for different integration step sizes

Step size (s)	$E - E_0$ ($\text{kg} \cdot \text{m}^2 \cdot \text{s}^{-2}$)
10^{-4}	1.98×10^{-9}
10^{-3}	1.11×10^{-7}
10^{-2}	1.09×10^{-2}

5. CONCLUSION

The dynamics of a helicopter underslung system consisting of two rigid bodies interconnected by cables are modelled using Kane's method. This formulation can be used to optimize the configuration of such a system for minimizing the dynamic interaction with a helicopter. The derivation uses the matrix form of Kane's equation, which has a distinct advantage over the widely published symbolic manipulation. The paper also describes the modelling of massless rigid bodies in the matrix form of Kane's equation. Even though the simulation results pertain to a particular configuration of the underslung system, a variety of configurations can be designed in order to optimize the system, based on this basic structure by judicious selection of the parameters listed in table 1.

The validation of the model without dissipative forces is established by verifying that the total mechanical energy of the system remains conserved. It is also seen that the choice of integration step size for fixed-step integration schemes like Runge-Kutta 4th order method is critical for this particular model due to the presence of massless rigid bodies in the system. Even though the results presented in this paper neglect aerodynamic forces, the formulated model provides for the inclusion of such forces.

REFERENCES

Cicolani, Luigi, S. and Ehlers, George, E. (2002). Modeling and simulation of a helicopter slung load stabilization device. URL <https://calhoun.nps.edu/handle/10945/60141>.

Enciu, J. and Rosen, A. (2014). Simulation of coupled helicopter-slung load-pilot dynamics. In *70th American Helicopter Society International Annual Forum 2014*, Annual Forum Proceedings - AHS International, 335–361. American Helicopter Society, United States.

Henderson, D. (1977). Euler angles, quaternions, and transformation matrices – working relationships. *National Aeronautics and Space Administration, Mission Planning and Analysis Division, Washington, DC*.

Kane, T.R. and Levinson, D.A. (1985). *Dynamics, theory and applications*. McGraw Hill.

Oktay, T. and Sultan, C. (2013). Modeling and control of a helicopter slung-load system. *Aerospace Science and Technology*, 29(1), 206–222.

Purushotham, A. and Anjeneyulu, M.J. (2013). Kane's method for robotic arm dynamics: a novel approach. *IOSR Journal of Mechanical and Civil Engineering*, 6(4), 7–13.

Rambely, A.S., Halim, N.A., and Ahmad, R.R. (2012). A numerical comparison of Langrange and Kane's methods of an arm segment. In *International Journal of Modern Physics: Conference Series*, volume 9, 68–75. World Scientific.

Sandino, L., Bejar, M., and Ollero, A. (2011). Tutorial for the application of Kane's method to model a small-size helicopter. In *Proceedings of the 1st Workshop on Research, Development and Education on Unmanned Aerial Systems*, 162–173.

Sivan, K. and Pandian, S. (2018). An overview of Reusable Launch Vehicle Technology Demonstrator. *Current Science (00113891)*, 114(1).

Stoneking, E. (2013). Implementation of Kane's method for a spacecraft composed of multiple rigid bodies. In *AIAA Guidance, Navigation, and Control (GNC) Conference*, 4649.

Thanapalan, K. (2016). Stability analysis of a helicopter with an external slung load system. *Journal of Control Science and Engineering*, 2016.

Tsukamoto, T., Yanagihara, M., Nagayasu, M., Sagisaka, M., Tsukamoto, T., Yanagihara, M., Nagayasu, M., and Sagisaka, M. (1997). ALFLEX five degrees of freedom hanging flight test. In *22nd Atmospheric Flight Mechanics Conference*, 3484.